

## MONTE CARLO SIMULATION OF THE MOBILITY IN QUASI-ONE-DIMENSIONAL SYSTEMS DISCOTIC LIQUID CRYSTALS

---

*Lazaros K. Gallos*

*Department of Physics, University of Thessaloniki, 54421,  
Thessaloniki, Greece*

*Bijan Movaghar*

*SOMS Centre, Department of Chemistry, University of Leeds,  
Leeds LS2-9JT, United Kingdom*

*L. Siebbeles*

*IRI Delft University of Technology, Mekelweg 19,  
2629 JB Delf, The Netherlands*

*The many-body Monte-Carlo method is used to evaluate the frequency dependent conductivity and mobility per carrier of a systems of electronic hopping charges moving on a one-dimensional chain or channel of finite length representing a discotic liquid crystal column. The concentration of charge  $N$  is varied using an imaginary gate electrode. In the liquid crystalline phase, we find that the electron-electron interaction reduces the mobility monotonically with density. Electron-electron interactions without disorder on the column only produce a weakly frequency dependent mobility. However, when interactions are combined with an injection barrier or intrinsic disorder, the free volume is reduced and the effects of disorder are amplified by interactions.*

### INTRODUCTION

The purpose of this paper is to understand how electron-electron interactions affect the ac conductivity in the static regime of transport in low dimensional material. Transport in one-dimensional or quasi one-dimensional molecular wires formed with self-assembled discotic molecules

One of the authors B. Movaghar, would like to thank NEDO (New Energy Development Organisation) Int. Joint Research Grant, for financial support.

Address correspondence to Lazaros K. Gallos, Department of Physics, University of Thessaloniki, Thessaloniki, 54421, Greece.

[1–3], nanotubes [4,5], and MBE gate engineered confined charged channels, constitutes currently a very hot and technically important topic [6]. Smectic liquid crystals constitute 2-dimensional self-organising liquids and represent another important area of transport physics [7,8]. Many ac response phenomena in conjugated polymers [9] and molecular wires have, we believe, in the past, been probably wrongly attributed to pure disorder, which are actually a result of electron-electron interactions. Electronic interactions come into play with high charging levels, such as occurs for example in electrode or gate charged FET organic interface and thin film transistor TFT. The same applies to highly doped materials. Charging energy is particularly important in high band gap, low dielectric constant and low-dimensional molecular materials such as smectic [7,8] and discotic liquid crystals [1,10–12].

Charges can be injected into organic materials chemically or by high fields and by light, and one can measure the frequency dependent conductivity [1,7–10]. The frequency dependent conductivity is in principle one of the easiest ways of seeing the effect of interactions, because the long range coulomb forces produce naively speaking, disorder-like potentials which confine and scatter the carriers and generate a frequency dependence on the motion which looks similar to the one produced by disorder. The problem in practice is, however, that one always has some disorder and some electrode polarization effects and then it is difficult to disentangle these processes from each other.

One the most exciting current areas of research is the study of injection and transfer of charge through large complex molecules. Present work is focusing on one-body tunneling and many workers are investigating the tunneling energy dependence [14]. We are here developing the tools to study the effect of Coulomb interactions on such process. The aim is to combine interactions with topological and orbital complexity [14].

## II. THE COMPUTATIONAL MODEL

Using many particle Monte Carlo, we study the effect of charge-charge interactions on the ac conductivity of finite and electrode addressed one-dimensional chains following the work in Ref [13]. A schematic representation of the system is shown in Figure 1. We consider that a molecular columnar wire, which does not interact with its neighboring columns, is charged via a gated electrode and is attached to two metal electrodes, which serve the purpose of source and drain. The gate electrode lies at a distance of  $d = 1$  nm from the column, and its distance from the edge electrodes equals  $L_G = 1.4$  nm. We have also considered the more realistic situation that the gate electrode is 30 nm away from the column. The

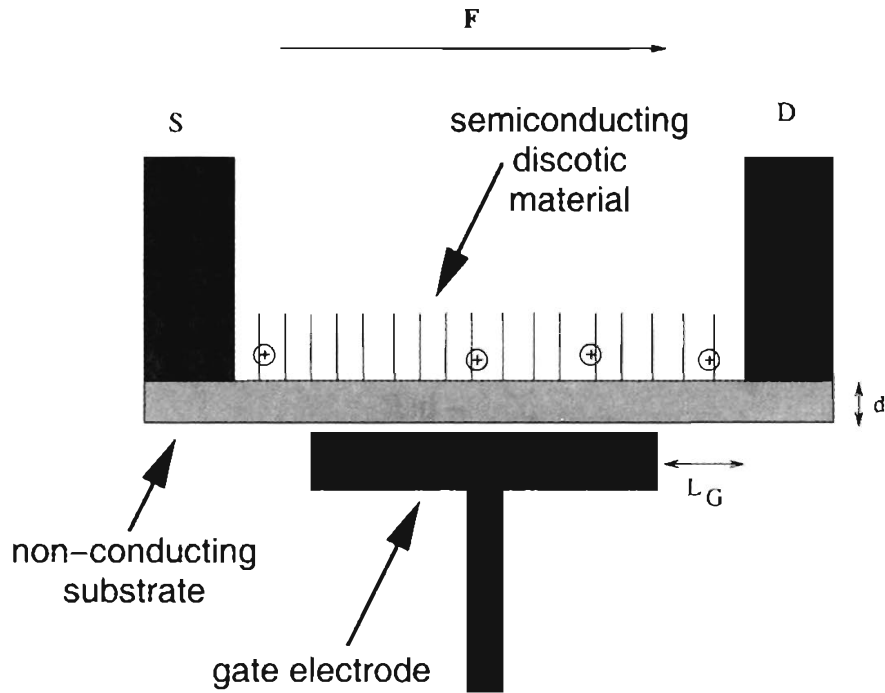


**FIGURE 1** Schematic diagram of the gated model system.

charges created in the column move along its length under the influence of an externally applied field, which can be either DC and AC. Charge can enter or leave the column through the metal electrodes where they build a steady state distribution.

In practice, we consider a column of 300 sites which corresponds to a 0.1 micron device. Initially, the number  $N$  of charges in the gate is defined, and we assume that the negative voltage at the gate causes an equal number of charges to appear in random positions in the column. During each step, the transition probabilities for all the charges in the column are computed, so that a charge in site  $n$  has a hopping transition rate  $W_{n,n\pm 1}$  towards its neighbors

$$W_{n,n+1} = \begin{cases} v_0 \exp\left(-\frac{\Delta E_{n,n+1}}{kT}\right) & \text{for } \Delta E_{n,n+1} > 0 \\ v_0 & \text{for } \Delta E_{n,n+1} \leq 0 \end{cases}, \quad (1)$$

where  $\Delta E_{n,n-1} = V_{n\pm 1} - V_n \mp eFa$ . The jump frequency  $v_0$  is fixed to  $10^{12}$  Hz. This corresponds to a typical phonon modulation frequency,  $V_n$  denotes the total Coulomb energy of a hole located on site  $n$ , which is due to the repulsive interactions caused by all other holes in the column plus the attractive energy corresponding to the presence of the gate, which is given by Eq. (4) in [13]. The distance  $a$  between two sites is constant and equal to 0.35 nm. The external electric field  $F$  can either be constant

$F_0 = 20$  kV/cm, or oscillating with a period  $\omega$ , so that  $F(t) = F_0 \cos(\omega t)$ . For the first and last site of the column the quantity  $\Delta E$  is modified, since now there is only one neighbour to move to, and injection/absorption to the electrodes is possible. The corresponding equations are given by Eqs. (5b)–(5e) in [1] ( $E_b$  denotes the energy barrier height between the organic material and the metal electrode).

Once the transition probability have been computed for all holes in the system, the time  $\delta t$  required for each hop is drawn by an exponential distribution, so that

$$\delta t = \frac{-\ln R}{W_{n,n+1} + W_{n,n-1}}, \quad (2)$$

with  $R$  being a uniformly distributed random variable. The shortest time of this ensemble (including the time needed for injection/absorption) is chosen and this jump takes place. The total time advances by the same amount, and the direction of the jump is decided with a probability

$$P_{n,n\pm 1} = \frac{W_{n,n\pm 1}}{W_{n,n-1} + W_{n,n+1}}. \quad (3)$$

The above procedure is repeated many times with the holes moving around, leaving and entering the column. In order to eliminate any initial distribution bias, we repeat the whole algorithm for a number of different realisations, with different random initial configurations. During all these realisations we monitor the average of the holes mobility  $\mu$  in the system with time, until this average is well converged.

The average hole mobility  $\mu$  is calculated via the work  $\Delta A$  done on all holes during an oscillation period  $\Delta t = 2\pi/\omega$ , and is given by

$$\mu = \frac{2\Delta A}{eF_0^2 \Delta t N_h}, \quad (4)$$

where  $N_h$  is the number of holes in the column.

### III. RESULTS

#### A. DC Mobility

In Figure 2 we present the mobility per hole for the gated system system under the influence of a DC field  $F = 20$  kV/cm, as function of the number of charges  $N$  in the gate. The energy barrier height is equal to  $E_b = 0.21$  eV. Different curves correspond to runs at different temperatures. We can see that in general, the mobility increases significantly with temperature, up to 3 orders of magnitude or more in the temperature range 100–300 K. The

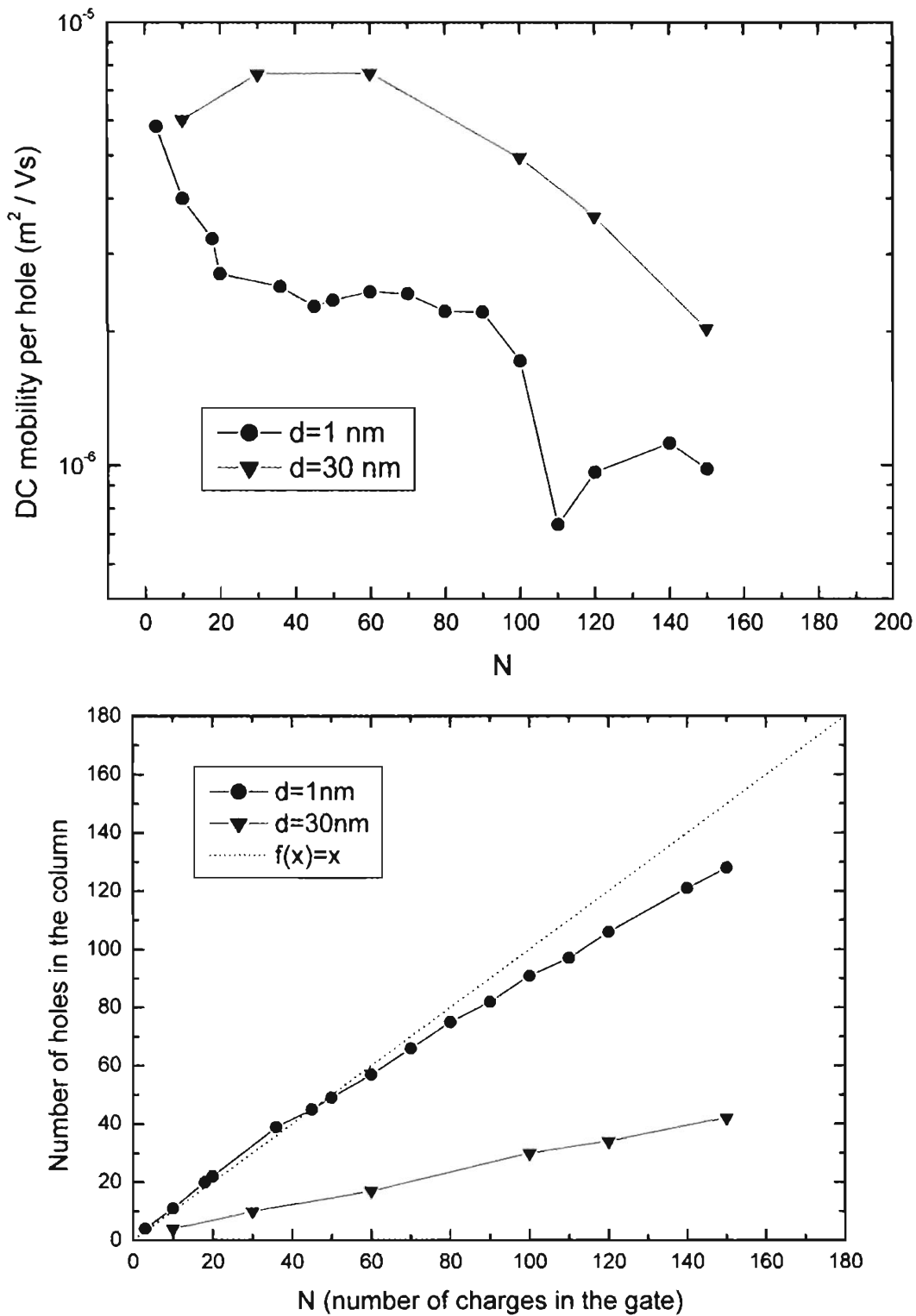


**FIGURE 2** a) The mobility per hole as a function of the average number of charges  $N$  in the column, for  $T = 300\text{ K}$ , under the influence of a  $20\text{ kV}$  DC field in two gate geometries  $d = 1\text{ nm}$  (ultra thin insulator) and  $d = 30\text{ nm}$  (conventional oxide thickness) b) The number of charges in the column as a function of  $N$  under the same conditions.

effective activation energy depends on the number of injected charge  $N$ . The increase in mobility with temperature is due to two factors. The carriers find it easier to come into the chain, and as the temperature increase, the charges can also hop more easily inside the chains against the field of other carriers. At temperatures of  $T = 50$  K and below, the charges are practically immobile and cannot overcome the charge-charge interaction barrier which keeps them vibrating around their stationary positions.

When the temperature is constant, Figure 3 shows that the mobility per hole decreases with increasing  $N$ . This is because the carriers have less space to move in. This is true for room temperatures and above, but this trend is violated at lower temperatures (not shown and to be published). For the present liquid crystal crystal applications which are at higher temperatures, the results are much easier to understand. In this regime, the charges have enough energy to overcome the local energy barriers pinning potentials. In the quasi-steady-state, at a given temperature, the actual number of carrier on the column need not correspond to the ideal number as calculated from the metallic Gate capacitance. The real number is shown in Figure 4. For the  $E_b$  value used, the average number of holes in the column during the simulation is close to the value expected from the gate charge except of course when we use the counter-ion distance  $d = 30$  nm. Here, the coulomb repulsion keeps “charges” out of the column (see Fig. 3). For  $d = 1$  nm, the gate to charge density matching is roughly one to one for all temperatures, and this is also true at the lower end of concentrations. At higher concentrations, we observe a reduction in the average number of holes in the column of the order of 10–15%, e.g. for  $N = 100$  expected, we have around 90 holes. For a realistic gate of  $d = 30$  nm, the charging is obviously much lower than “the ideal capacitance value” which assumes metallic screening in the charging electrode.

## B. AC Mobility

### *Finite Electrode Barrier Height*

The ac conductivity is shown in Figure 4 for 3 different temperatures. We observe an increase in the dispersion as we go from low  $N$  to an intermediate  $N$ . This is a many-body effect and is related to the pinning of charge i.e. a change in the injection and absorption efficiency which is caused by the Coulomb interactions. The increase in charge density restricts the free space and lowers the average mobility. A real time study shows that at high  $N$ , the carriers undergo a sequential “billiard ball” type transfer process, where one carrier enters on the “left” when one has exited from the “right”. Beyond the density delimited by the “Coulomb radius”, when n.n interaction energies are larger than  $kT$ , the shape of the frequency curves is relatively insensitive to the magnitude of  $N$ .

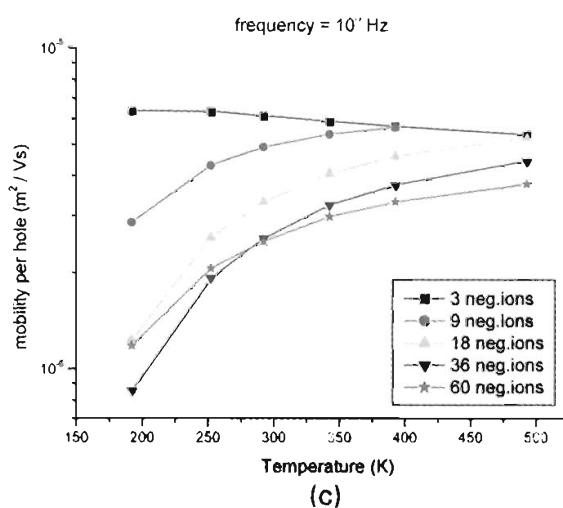
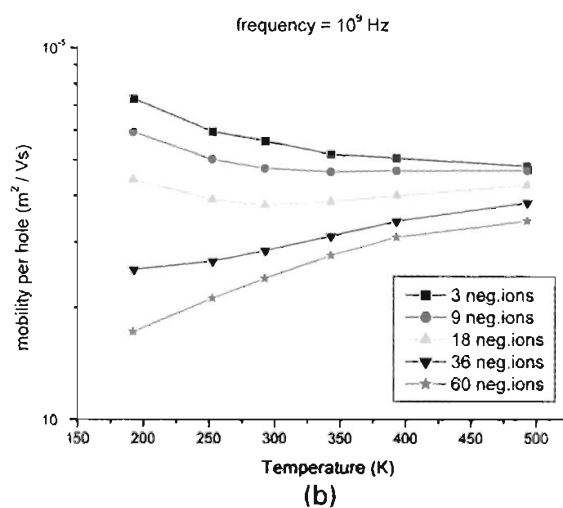
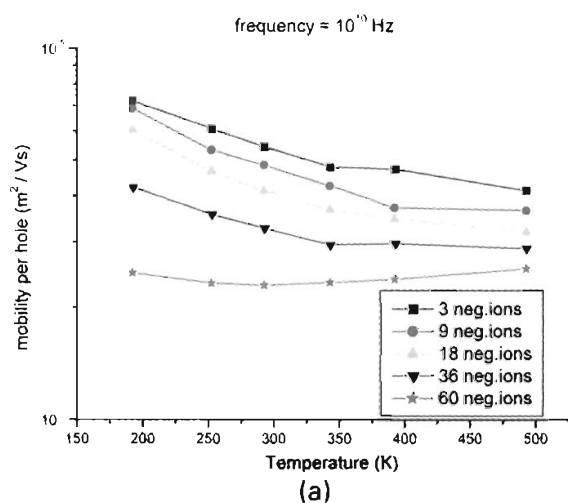


**FIGURE 3** Temperature dependence of the AC mobility per hole for different initial charge concentrations and field frequencies: a)  $10^{10}$  Hz, b)  $10^9$  Hz and c)  $10^6$  Hz. Top to bottom:  $N = 3, 9, 18, 36, 60$ . The injection barrier height of the electrode is equal to 0.21 eV.

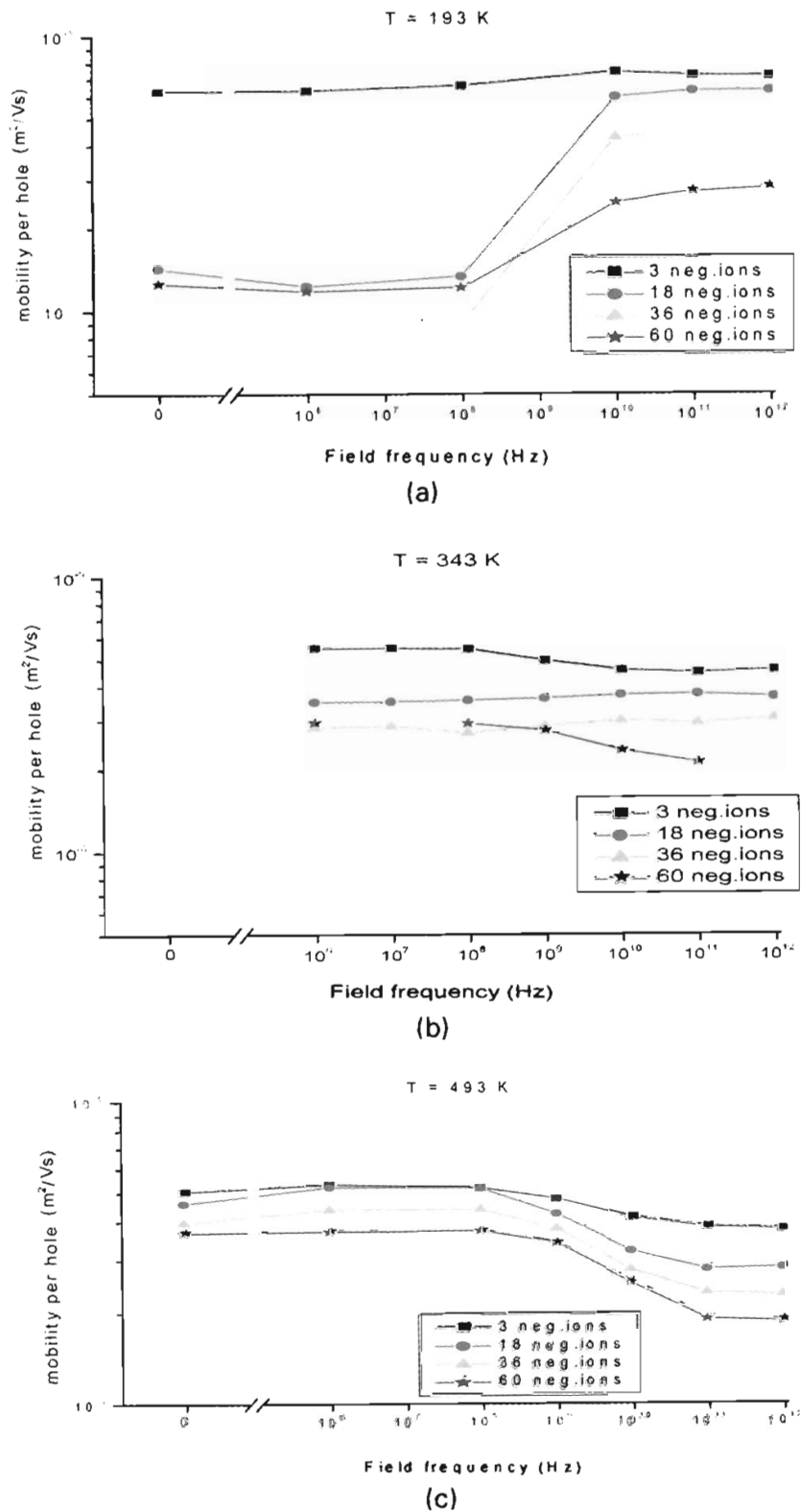


**FIGURE 4** Variation of the AC mobility per hole with the field frequency. The injection barrier height of the electrode is equal to 0.21 eV. Three different temperatures are presented: a)  $T = 193 \text{ K}$  and b)  $T = 343 \text{ K}$  and c)  $T = 493 \text{ K}$ . Top to bottom:  $N = 3, 18, 36, 60$ .



At very high temperatures, the ac mobility actually decreases with frequency at high frequencies. This is due to the fact that carriers are now forced to oscillate in a smaller volume, whereas at lower frequencies there are many-body (“sequential in phase”) Pathways, which allow carriers to cross the sample and these contribute more to the displacement.

#### IV. CONCLUSIONS

We have studied the charge transport in interacting quasi-one dimensional charged systems with emphasis on the temperature dependence of the mobility. We have seen that the mobility is temperature dependent and in the range of interest for columnar liquid crystal applications, the temperature dependence is mainly due to the presence of the injection barrier with a small contribution coming from electron-electron interactions. At low temperatures we have a very small hole mobility mainly because of the injection barrier. Cooperative effects in the temperatures range of interest come into play mainly to lower the mobility by reducing the effective free volume, this is shown in Figure 3. The temperature dependence is partially due to the assumed injection barrier and partially due to the fact that at high  $N$ , carriers have to “push their way in” like a line of colliding billiard balls”. Both factors work together to produce the final result shown in Figure 2.

In hopping systems, the frequency dependence of the mobility is in general due to a distribution of hopping speeds with the slow hops showing up at low frequencies and the fast hops at high frequencies. In a one-body situation the frequency dependence, is then mainly a manifestation of disorder. In the interacting electron-gas case, three changes occur a) interactions lower the average mobility and b) interactions, injection rates and thermal excitations cause changes in the steady state charge density, and this in turn affects the average mobility via process a), and finally c) interactions, when combined with specific electrode geometries and injection barriers can produce  $N$ -dependent charge-pinning. Charges adopt the order which minimizes the coulomb energy. This produces a characteristic hopping time distribution and thus a many-body ac response. In one dimension, with densities beyond the Coulomb radius, the transport paths are mainly sequential and this makes the onset of the frequency dependence in the ac current relatively insensitive to the density  $N$ . Therefore, the ac response data on p-doped HAT6 can, unfortunately, not be simply related to interactions. They occur at much lower frequencies as predicted here and can only be understood when both interface/disorder and interactions are taken into account. Interactions reduce the free volume and enhance the effect of simple blockages. The modeling has to include both aspects. In 2-dimensional systems we expect interactions to be to first

approximation quite like disorder potentials. The tools that we have developed will allow us to investigate this and also to design device topologies which exhibit a desired type of ac response.

## REFERENCES

- [1] (a) Boden, N., Bushby, R. J., Borner, R. J., Cammidge, R. C., & Jesudason, M. W. (1993). *Liq. Cryst.*, *15*, 851.  
 (b) Boden, N., Bushby, R. J., Clements, J., & Movaghar, B. (1995). *J. Appl. Phys.*, *33*, 3207.  
 (c) Arikainen, k., Boden, N., Bushby, R. J., Clements, J., & Movaghar, B. (1995). *J. Mat. Chem.*, *5*, 2161.
- [2] (a) Adam, D., Closs, F., Frey, T., Funhoff, D., Haarer, D., Ringsdorf, H., Schumacher, P., & Siemensmeyer, S. K. (1993). *Phys. Rev. Lett.*, *70*, 457  
 (b) Bacher, A., Bleyl, I., Erdelen, C. H., Haarer, D., Paulus, W., & Schmidt, H. W. (1997). *Adv. Mater.*, *9*, 1031.
- [3] Boden, N., Clements, J., Bushby, R., Donovan, K., & Kreouzis, (1995). *Phys. Rev. B*, *52*, 13–274;(1998). *Phys. Rev. B*, *158*, 3063;(2002). *Phys. Rev. B*, March 15 vol.
- [4] Yao, Z., Postma, H. W. Ch, Balents, L., & Dekker, C. (1999). *Nature*, *402*, 273.
- [5] (a) Boden, N. & Movaghar, B. (1998). In: *Liquid Crystal Handbook*, Demus, D., Goodby, J. W., Gray, G. W., Spiess, H. W., & Vill, V. (Eds.), Wiley-VCH, Vol. *2B*, 781.  
 (b) Carroll, D. L., Kinlen, P., Raman, S., Redlich, Ph., Rühle, M., Blas, X., Charlier, J.-C., Curran, S., Roth, S., & Ajayan, P. M. (1997). Kuzmany, H., Fink, J., Mehrihg, F., & Roth, S. (Eds.), World Scientific: Singapore, 477;(1998). *Carbon*, *36* (5–6), 753.
- [6] Rother, M., Wegscheider, W., Ertl, F., Deutschmann, R., Bichler, M., & Abstreiter, G. (1999). *Microelectronics*, *47*, 215.
- [7] Funahashi, M. & Hanna, J. (2000). *Appl. Phys.*, *76*, 2574.
- [8] Funahashi, M. & Hanna, J. (1999). *Mol. Cryst. Liq. Crystals*, *331*, 509.
- [9] Ribo, J., Anglada, M. C., Hernandez, J. M., Zhand, X., Ferrer-Anglada, N., Chaibi, A., & Movaghar, B. (1998). *Synthetic Metals*, *97*, 229.
- [10] Schoen, J. H. (2001). *Nature*, *410*, 8 March.
- [11] Schoen, J. H., Kloc, Ch, & Batlogg, B. (2001). *Science*, *293*, 2432.
- [12] (a) Service, R. F., Moerner, We, Orrit, M., Weiss, S., G. J. K., & Joachimin, C. (1999). *Science*, *283*, 1667.  
 (b) Chen, J., Reed, M. A., Rawlett, A. M., & Tour, J. M. (1999). *Science*, *286*, 1550  
 (c) Dekker, C. & Ratner, M. (2001). *Physics World*, *14*, 29.
- [13] Siebbeles, L. D. A. & Movaghar, B. (2000). *J. Chem. Phys.*, *113*, 1609.
- [14] (a) Zhou, C., Newns, D. M., Misewich, J. & Pattnaik, P. C. (1997). *Appl. Phys. Lett.*, *70*, 598.  
 (b) Ouisse, T. & Billon, T. (1995). *Phil. Mag. B.*, *71*, 413.